Biochimica et Biophysica Acta 1847 (2015) 565–575

Contents lists available at ScienceDirect

Biochimica et Biophysica Acta

journal homepage: www.elsevier.com/locate/bbabio

Oxidation of plastohydroquinone by photosystem II and by dioxygen in leaves

Agu Laisk *, Hillar Eichelmann, Vello Oja

Tartu Ülikooli Tehnoloogia Instituut, Nooruse tn. 1, Tartu 50411, Estonia

ARTICLE INFO

Article history:
Received 17 November 2014
Received in revised form 16 February 2015
Accepted 15 March 2015
Available online 20 March 2015

Keywords:
Leaves
Photosystem II
Cyclic electron transport

ABSTRACT

In sunflower leaves linear electron flow LEF = 4 O_2 evolution rate was measured at 20 ppm O_2 in N_2. PSII charge separation rate $CSR_{II} = a_{II}{\cdot}PAD{\cdot}(F_m - F) / F_m$, where a_{II} is excitation partitioning to PSII, PAD is photon absorption density, F_m and F are maximum and actual fluorescence yields. Under 630 nm LED + 720 nm far-red light (FRL), LEF was equal to CSR_{II} with $a_{II} = 0.51$ to 0.58. After FRL was turned off, plastoquinol (PQH_2) accumulated, but LEF decreased more than accountable by F increase, indicating PQH_2-oxidizing cyclic electron flow in PSII (CEF_{II}). CEF_{II} was faster under conditions requiring more ATP, consistent with CEF_{II} being coupled with proton translocation. We propose that PQH_2 bound to the Q_C site is oxidized, one e^- moving to $P680^+$, the other e^- to Cyt b_{559}. From Cyt b_{559} the e^- reduces Q_B^- at the Q_B site, forming PQH_2. About 10–15% electrons may cycle, causing misses in the period-4 flash O_2 evolution and lower quantum yield of photosynthesis under stress. We also measured concentration dependence of PQH_2 oxidation by dioxygen, as indicated by post-illumination decrease of Chl fluorescence yield. After light was turned off, F rapidly decreased from F_m to 0.2 F_v, but further decrease to F_0 was slow and O_2 concentration dependent. The rate constant of PQH_2 oxidation, determined from this slow phase, was 0.054 s^{-1} at 270 μM (21%) O_2, decreasing with $K_m(O_2)$ of 60 μM (4.6%) O_2. This eliminates the interference of O_2 in the measurements of CEF_{II}.

1. Introduction

Plastoquinone (PQ) is a lipid-soluble, diffusible in the membrane compound that stands on the central crossroad of photosynthetic electron transport pathways. The relative redox state of PQ acts as a sensor of environmental change [1], triggering various cellular responses [2], including modulated expression of genes that encode the light-harvesting apparatus of photosynthesis [3]. Plastoquinone can be stably reduced to form plastoquinol (plastohydroquinone, PQH_2) by accepting two electrons and two protons. The single-reduced radical semiquinone is relatively unstable (E_m of PQ/PQ^- is −170 mV [4]).

In photosynthesis the mainstream linear electron flow (LEF) through PSII reduces PQ, which accepts protons from the stroma, and PQH_2 is oxidized by donation of electrons to the Rieske Fe carriers in the cytochrome b_6f complex (Cyt b_6f), releasing protons into the thylakoid lumen. Such proton-coupled LEF is still insufficient to support the necessary >3ATP/2NADPH ratio requiring >$14H^+/4e^-$ [5], therefore, PQ is also reduced by two kinds of cyclic electron flow around PSI (CEF_I), returning to PQ a fraction of electrons once passed through the Cyt b_6f complex. The (minor) chloroplast NAD(P)H dehydrogenase-related route of PQ reduction was suggested by [6] and a novel protein component CRR31 is essential for the efficient operation of Fd-dependent plastoquinone reduction by this complex [7]. The (major) antimycin A-sensitive, ferredoxin-dependent PQ reduction pathway [8] is based on a PROTON GRADIENT REGULATION protein PGR5 [9,10]. PGR5 and a "PGR5-like" protein PGRL1 were found interacting physically and being associated with PSI [11], most probably representing the elusive ferredoxin:quinone reductase (FQR) enzyme [12,13], though evidence that Q_A, but not PQ, is the direct electron acceptor was recently published [14].

The mainstream photosynthetic pathway of PQH_2 oxidation goes via the Q-cycle located in the Cyt b_6f complex, followed by light-supported electron transport through PSI. In this work, however, we focus on alternative processes oxidizing plastoquinone. PQH_2 does not remain reduced post illumination in the dark, but slowly becomes oxidized by oxygen via plastid terminal oxidase (PTOX) activity, as well as non-enzymatically by superoxide radical. Initially, PSI-less mutants of *Chlamydomonas reinhardtii* and *Chlorella pyrenoidosa* were shown to be able for oxygen-dependent PQH_2 oxidation by an enzyme that is located in electron transport chain between PSII and Cyt b_6f [15].

Abbreviations: AL, actinic light; a_{II}, relative optical cross-section of PS II; CEF, cyclic electron flow; CSR, charge separation rate; Cyt b_6f, cytochrome b_6f; $Cytb_{559}$, cytochrome b_{559}; ETR, electron transport rate; FRL, far-red light; FNR, ferredoxin:$NADP^+$ reductase; F_m, F, F_r, F_0, fluorescence yields, maximum, actual, residual and minimal; LED, light-emitting diode; LEF, linear electron flow; PFD, PAD, photon flux density, incident and absorbed; PSI, PSII, photosystems II and I; PQ, PQH_2, plastoquinone, oxidized and reduced; PTOX, plastid terminal oxidase; P680, donor pigment complex of PS II; Q_A, Q_B, Q_C, quinone binding sites in PS II; Tyr Z, tyrosine Z; Y_{III}, global quantum yield of PSII for LEF; y_{III}, yield of linear electron flow

* Corresponding author.
E-mail address: agu.laisk@ut.ee (A. Laisk).

http://dx.doi.org/10.1016/j.bbabio.2015.03.003
0005-2728/

An important finding was that in an *Arabidopsis* mutant IMMUTANS showing a variegated phenotype [16,17] the inactivated gene led to an impairment in phytoene desaturation, an essential step in carotenoid biosynthesis that requires PQ as an electron acceptor. In the mutant PQH_2 did not become sufficiently oxidized in the dark to be able to support carotenoid synthesis. Since the inactivated gene possessed sequence homologies with mitochondrial alternative oxidases, the IMMUTANS (IM) gene was named PTOX for plastid terminal oxidase [18,19]. PTOX is a 37 kDa nuclear-coded protein present in organisms that exhibit oxygenic photosynthesis [16,17] bound mostly to stroma thylakoids in a quantity of 1 PTOX per 100 PSII [20,21]. PTOX is a non-heme di-iron oxidase that can utilize plastoquinol, but not ubiquinol as a substrate [22], the end product of the oxygen reduction step being water [18]. As to the physiological role, it was proposed that PTOX may act as a "safety valve" or alternate electron sink to dissipate excess energy that might accumulate in the absence of fully functional electron transport chains in the early stage of chloroplast formation [17,23]. This model however was questioned in a study where the actual kinetics of PTOX were investigated in wild type and variegated tomato leaves [24]. In the dark, at 21% O_2 the maximum PTOX rate was smaller than 1 $e^-\ s^{-1}$ per PSII. Under all the conditions tested the enzyme activity always remained about two orders of magnitude lower than that of electron flux through the linear photosynthetic electron pathway. Therefore, PTOX generally cannot play a role of a safety valve for photo-generated electrons, though this is not excluded under stress conditions, e.g. when terminal electron acceptors are strictly limiting [25].

There is also a possibility for non-enzymatic oxidation of PQH_2, the chemistry involving activated intermediate forms of the substrates — semiquinone PQ^- and superoxide O_2^- radicals [4,26]. Oxidation of the PQ-pool after illumination with 50 or 500 μmol quanta $m^{-2}\ s^{-1}$ was measured in isolated pea thylakoids spectrophotometrically as the increase in ΔA_{263}, i.e., as the appearance of PQ. PQH_2 did not oxidize in the dark in the absence of oxygen, but under 21% O_2 the oxidation was biphasic. The authors concluded that a plastoquinone oxidase could not be involved in the biphasic process, but the initial fast phase was caused by superoxide, initially accumulated in thylakoids during illumination [27], the slow phase continuing autocatalytically.

Another interesting route has been suggested that plastoquinol might be oxidized by electron transfer to cytochrome b_{559} — a heme in the PSII complex whose metabolic function is not yet clear [28]. Though the participation of PTOX was not completely excluded in these experiments, the detected parallel redox changes in PQ and Cyt b_{559} remain a fact. By testing different quinones, rather low structural quinone specificity was observed for the Cyt b_{559} quinone-catalyzed photoreduction, the data favoring the view that the quinone-binding site active in Cyt b_{559} photoreduction is a Q_C site, different from the Q_A and Q_B sites in PSII [29].

Rather than oxygen being the terminal electron acceptor, these data are consistent with the PSII cycle, where photo-oxidized $P680^+$ is the electron acceptor. Cycling of electrons around PSII has been detected [30] in thylakoid membranes [31] and chlorella cells [32], but in leaves the fast rates detected at high light intensities have been related to donor side charge recombination rather than electron cycling via the PQ pool [33–35]. The slow cyclic pathway is based on photo-oxidation of Cyt b_{559} as follows: Cyt $b_{559} \rightarrow Car_{D2} \rightarrow Chl_{D2} \rightarrow P680^+$ [36–39]. The photo-oxidized Cyt b_{559} is re-reduced either by the PSII-bound reduced Q_B [40] or by the diffusible PQH_2 [29,41].

The physiological role of CEF_{II} involving Cyt b_{559} is still not clear, mainly because for technical reasons investigations of the secondary electron transport pathways within PSII have been carried out almost exclusively on isolates lacking the complete functional electron transport pathway. In this work we have used intact leaves possessing fully competent electron transport chain, and applied precise methods for leaf gas exchange and Chl fluorescence measurements, facilitating detection of small differences between the rates of charge separation rate within PSII (CSR_{II}), detected from Chl fluorescence, and linear electron flow through PSII (LEF), detected from O_2 evolution. The small but experimentally significant difference between CSR_{II} and LEF indicates that a part of electrons once transferred through PSII do not continue the traffic along the linear pathway, but return to the donor side of the photosystem. The cyclic process is faster in circumstances where faster extra ATP synthesis is required. We propose a mechanism for this CEF_{II}, which, similarly to the Q-cycle, is based on sequential double oxidation of one and double reduction of the other plastoquinone, using Cyt b_{559} and Q_B^- for temporary storage of the second electron.

In order to evaluate the competitive pseudo-cyclic electron turnover via PQH_2 oxidation by O_2 in our experiments, we also measured the O_2 concentration dependence of the post-illumination oxidation of intersystem electron carriers. It appears that the O_2 concentration requirement for this process is much higher than it was realistically available in our experiments. The actual rate of PQH_2 oxidation by dioxygen was by two orders of magnitude slower than the recorded rate of the light-dependent oxidation PQH_2 by PSII.

2. Materials and methods

2.1. Plant material

Sunflower (*Helianthus annuus* L.) plants were grown in a growth chamber in 4 l pots filled with peat-soil mixture with added NH_4NO_3, or an aeroponic growth system was used in the NO_3^-- or NH_4^+-nutritioned growth experiments [42]. Fully grown leaves attached to the plant were fitted to the leaf chamber for measurements.

2.2. Leaf illumination and gas exchange measurements

A laboratory-made two-channel leaf gas exchange measurement system [43] enabled control and measurement of CO_2, O_2 and water vapor concentrations (for performance see [44]). A 32 mm diameter and 3 mm thick leaf chamber, covering a part of the leaf, was illuminated by LED-based light sources through a multi-branched fiber-optic light guide (630 nm actinic, 720 nm far-red). Light intensity was measured with spectro-radiometer PC2000 (Ocean Optics, FL) calibrated against a standard lamp. The spectrum of leaf absorptivity was measured with the PC2000 in an integrating sphere and photon absorption density (PAD) was calculated by integration over the spectrum of LED emission intensity, μmol $m^{-2}\ s^{-1}\ nm^{-1}$, times leaf absorptivity. Rates of CO_2 exchange were measured with an infrared gas analyzer LI-6251 (LiCor, Lincoln, NE, USA), O_2 evolution was measured in the same gas flow with a zirconium O_2 analyzer S-3A (Ametek, Pittsburgh, PA, USA) on the background of 20 ppm O_2 in N_2 containing CO_2 as indicated. Both gas analyzers were precisely calibrated [45]. Response time of the O_2 measurement was 0.8 s and that of the CO_2 was 1.6 s.

2.3. Electron transport and quantum yields from gas exchange

Linear electron flow rates were calculated from CO_2 exchange at 21% O_2 using Eq. (1) [44],

$$LEF_C = 4(A_C + R_K)\frac{2K_sC_c + 2O_c}{2K_sC_c - O_c}, \quad (1)$$

where A_C is CO_2 gas exchange rate, R_K is Krebs cycle respiration, K_S is Rubisco specificity factor (98 at 22 °C), and C_C and O_C denote corresponding dissolved gas concentrations in chloroplast stroma. From O_2 exchange at 20 ppm O_2 LEF was calculated according to Eq. (2) equally for both photosystems

$$LEF = 4A_O, \quad (2)$$

where A_O is O_2 evolution rate. For CO_2 measurements down-regulation

of R_K in the light was modeled as in [42], for O_2 measurements the base line was determined in the dark, assuming nearly zero respiratory O_2 uptake at the used low O_2 concentration. PSII density, μmol m^{-2}, was measured as 4 times O_2 evolution from an individual saturating single-turnover flash, superimposed on FRL background [46].

The global (with respect to total absorbed light) quantum yield of LEF, Y_{IIL}, was calculated as

$$Y_{IIL} = \mathrm{LEF}/\mathrm{PAD} \tag{3}$$

using LEF from Eqs. (1) or (2). In the − FRL measurements PAD was the absorbed 630 nm LED light, + FRL was considered as an equivalent 630 nm light causing as fast additional O_2 evolution as the used FRL (3.5 ± 0.3 μmol e^- m^{-2} s^{-1}).

2.4. Chlorophyll fluorescence measurements

In steady-state light curves Chl fluorescence was measured with a PAM-101 and ED-101 emitter-detector (H. Walz, Effeltrich, Germany). For F_m, dual-intensity saturation pulses were applied (7300 μmol m^{-2} s^{-1} for 300 ms, 3300 for 300 ms) and the true F_m was obtained by extrapolation to an infinite light intensity. PSI fluorescence, constantly 37% of F_0 [47], was subtracted from F and F_m. PSII charge separation rate was calculated as

$$\mathrm{CSR} = a_{II} \cdot \mathrm{PAD} \cdot (F_m - F)/F_m, \tag{4}$$

where a_{II} is excitation partitioning ratio to PSII and PAD is photon absorption density. The global quantum yield of linear electron flow through PSII was expressed from fluorescence data as follows:

$$Y_{IIL} = a_{II} y_{IIL} (F_m - F)/F_m, \tag{5}$$

where y_{IIL} is the "yield" of linear flow with respect to PSII charge separation. Considering the expressions for Y_{IIL} from gas exchange (Eq. (3)) and from Chl fluorescence (Eq. (5)) we compose the following expression, which is the slope of the line in the "yield" plot:

$$\frac{Y_{IIL}}{(F_m - F)/F_m} = a_{II} y_{IIL}\,, \tag{6}$$

where the left side contains only measured values, allowing us to find excitation partitioning to PSII under conditions where the PSII cycle (y_{IIL}) could be considered zero or constant. Electron cycling rate around PSII, CEF_{II}, was calculated as difference between PSII charge separation rate (Eq. (4)) and LEF rate (Eq. (2)):

$$\mathrm{CEF}_{II} = \mathrm{CSR}_{II} - \mathrm{LEF} \tag{7}$$

2.5. Fluorescence induction and yield decay measurements

In these measurements fluorescence was induced by a high actinic light of 4000 μmol m^{-2} s^{-1} (630 nm). Fluorescence was excited by the same light and computer-recorded through a set of filters in the spectral window of 720 to 760 nm [35]. After reaching F_m actinic light was turned off and the decay of fluorescence yield was recorded with PAM 101 at the low excitation frequency of 1.6 kHz. Complementary area of fluorescence induction was calculated as in [35], and the induction curves were plotted against the gradually increasing complementary area, which is equivalent to the number of photochemically quenched photons plotted on the abscissa.

2.6. O_2 concentration in chloroplasts

O_2 concentration in chloroplasts was calculated from the unidimensional steady-state diffusion equation

$$A_O = \frac{O_c - O_{wl}}{r_l} = \frac{O_{wg} - O_a}{r_g} \tag{8}$$

$$O_{wl} = \beta \cdot O_{wg} \tag{9}$$

where A_O is the measured rate of O_2 evolution, μmol m^{-2} s^{-1}, O is O_2 concentration, μM, as indicated by subscripts: c, in chloroplast; wl in liquid at the cell wall; wg, in gas at the cell wall; a, in ambient gas. Diffusion resistances r are expressed in units s mm^{-1} (instead of s dm^{-1}) in order to be consistent between the used concentration units, μmol dm^{-3}, and flux units, μmol m^{-2} s^{-1}. Solubility of O_2 in water was considered as the Henry constant $\beta = 0.032$, molar in liquid vs. molar in gas at 22 °C. Eqs. (8) and (9) yield the following expression for O_C:

$$O_C = \left(r_l + \beta r_g\right) A_O + \beta O_a. \tag{10}$$

The gas phase resistance was determined for water vapor from transpiration using common methods [48,49] and converted for O_2 multiplying by 1.33 (square root of the ratio of molar masses of O_2 and H_2O). The liquid phase resistance (mesophyll diffusion resistance) was measured 0.012 s mm^{-1} for CO_2 in sunflower leaves [44,50], divided by 1.17 to obtain the value 0.010 ± 0.0006 s mm^{-1} for O_2.

3. Results

3.1. CEF_{II} is induced by reduced plastoquinone

In sunflower leaves the light response curve of net CO_2 fixation was measured under 630 nm LED actinic light, AL, with added FRL as shown in Fig. 1A. With AL + FRL the steady-state Chl fluorescence yield F decreased, approaching F_0 at PAD < 500 μmol m^{-2} s^{-1}, indicating oxidation of PQH_2 due to the high PSI activity supported by FRL. At low actinic PADs this pattern of F significantly changed while FRL was turned off for 40 s: F increased since PSII was slightly overexcited compared with PSI at 630 nm, causing accumulation of PQH_2 and related increase in Q_A reduction due to the reversible binding of PQH_2 to the Q_B site [51].

For further analysis LEF rate was calculated from the net CO_2 uptake rate (Eq. (1)) and the global quantum yield of LEF, Y_{IIL}, was calculated as (electrons used for photosynthetic CO_2 uptake and photorespiratory CO_2 evolution) per (actinic photon absorbed in the leaf). The role of FRL was considered through its "630 nm equivalent" causing as much O_2 evolution as FRL [52] (see Materials and methods). In Fig. 1B the so calculated quantum yield of photosynthetic electron flow is plotted against the quantum yield of PSII charge separation as detected from Chl fluorescence. This "yield plot" conveniently indicates excitation partitioning to PSII and photon losses in processes accompanied by fluorescence, as well as in processes not accompanied by fluorescence.

If the quantum yield is controlled only by fluorescence-indicated losses then data points would form a straight line beginning with zero yield at $F = F_m$ (high PADs). At $F \to 0$ (low PADs) the straight line extrapolates to a maximum yield no more involving F-indicated losses. Therefore, at $F = 0$ the global yield $Y_{IIL} = a_{II} \cdot y_{II}$, where a_{II} is the coefficient indicating partitioning of excitations to PSII and y_{IIL} is another "yield" coefficient indicating the probability that an electron, separated from the donor P680 as a result of the photochemical quenching of a photon, successfully arrives at the terminal acceptor of LEF. Evidently, cycling of electrons back to $P680^+$ is indicated by $1 - y_{IIL}$. This extrapolated value of the global yield $Y_{IIL} = a_{II} \cdot y_{IIL}$ at $F = 0$ is our experimental

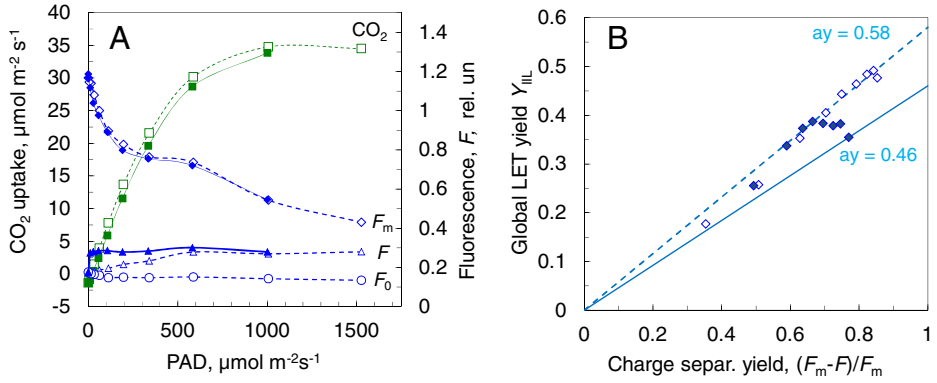

Fig. 1. A: Light response curves of net CO_2 exchange rate and Chl fluorescence parameters F_0, F and F_m in a sunflower leaf. The leaf was illuminated with 630 nm actinic light plus 720 nm far-red light of 20 μmol m^{-2} s^{-1} absorbed (AL + FRL) from higher to lower photon absorption densities (PAD), stabilizing the rate at each step for 2–3 min (dashed lines and open data points). At each step FRL was turned off for 40 s, sufficient to adjust photosynthesis to the lower PSI/PSII excitation balance (filled data points and solid lines). CO_2 concentration was 360 ppm, O_2 21%, temperature 22 °C. B: Yield plot from panel A. Linear electron flow (LEF) rate was calculated from the net CO_2 uptake rate (Eq. (1)), the global quantum yield of LEF, Y_{IIL}, was calculated in relation to the absorbed 630 nm light plus FRL (see Materials and methods) and plotted against the quantum yield of PSII charge separation $Y_{II} = (F_m - F)/F_m$. Extrapolation to the right ordinate ($F = 0$) indicates the product of the excitation partitioning factor to PSII, a_{II}, and the yield (probability) for separated charges to continue the linear flow to CO_2, y_{IIL} (Eq. (6)).

target in this work. For brevity we further denote it as *ay*, emphasizing that this measured parameter still is the product of two variables — excitation partitioning to PSII and electron cycling around PSII. We shall deconvolute these two variables using their different time dependence.

From the yield plot of Fig. 1B one can see that the + FRL data points measured at light limitation form a straight line indeed, extrapolating to $ay = 0.58$. Assuming that with + FRL there was no cycling of electrons around PSII and, thus $y_{IIL} = 1$, extrapolation revealed the excitation partitioning coefficient $a_{II} = 0.58$. The − FRL measurements however revealed an un-expected result: as soon as FRL was turned off, the data points moved to the left, indicating increased fluorescence due to the accumulation of PQH_2, but simultaneously declined downwards from the + FRL-defined *ay* line. It means, under the PSI-limited conditions PQH_2 level increased, accompanied by increased fluorescence, but PSII linear electron transport decreased more than explainable by the fluorescence rise. Linear electron transport through PSII was down-regulated by dual ways – first by increased Q_A reduction increasing fluorescence, but in parallel also by the decreased *ay* product, indicating either decreased LEF yield y_{IIL} — which would mean increased CEF_{II} – or/and decreased PSII antenna size a_{II} due to state transition-type movement of PSII antenna components. Below we show that the state transitions were not involved in this relatively fast process, thus, an acceptor side product of PSII electron transport was photochemically re-oxidized by PSII. This PSII cycle was relatively more pronounced at low PADs, when the used 630 nm light more strongly overexcited PSII compared to PSI. At higher PADs non-photochemical quenching inactivated PSII, balancing excitation or over-exciting PSI independent of the presence or absence of FRL. Nevertheless the two saturating-light data points indicate a lower *ay* value. Under very high light the lower y_{IIL} was caused by "donor side quenching" due to charge recombination [35]. In experiments below, carried out at saturating light intensities, we considered this component of y_{IIL} as constant and interpreted only changes in y_{IIL}.

3.1.1. The PSII cycle is running faster when more extra ATP is required

All the following experiments were carried out at the gaseous O_2 concentration of 20 ppm in order to minimize the role of oxygen as an alternative electron acceptor.

In order to test whether the PQH_2 oxidizing PSII cycle is related to photophosphorylation, we compared its rate under conditions where the necessity for extra ATP synthesis was potentially different. For this we used sunflower plants grown aeroponically with 3 mM NO_3^- or 3 mM NH_4^+, with an aim to elucidate the interaction of the PSII cycle with the presence or absence of nitrite as an alternative terminal electron acceptor. Light response curves were measured using the routine of Fig. 1A, but O_2 evolution was measured in the ambient O_2 concentration of 20 ppm. In the NH_4^+ plants the effect on *ay* of the PSII cycle was stronger than in the NO_3^- plants (Fig. 2A, B). Even the presence of FRL did not completely eliminate the activation of CEF_{II} in the NH_4^+ plants, as seen from the placement of the low PAD data points in Fig. 2B. On average in 8 sample plants the rate of CEF_{II} was about twice as fast in the NH_4^+ plants as it was in the NO_3^- plants (Fig. 2C). This result was consistent with the hypothesis that increased PSII CEF compensated for ATP, no more produced by electron flow to nitrite.

3.2. ATP produced by CEF_{II} supports recovery from over-reduction

Electrons accumulate and the photosynthetic electron transport chain becomes highly reduced under conditions where the stoichiometric ratio of ATP/NADPH production drops below the critical value, necessary for the phosphorylation of 3-phosphoglyceric acid at the rate equal to the rate of NADPH production. Such over-reduction occurs during dark-light induction [53–55] and during oscillations of photosynthesis [56,57]. Below we show that CEF_{II} is activated during recovery from over-reduction.

3.2.1. Induction

In Fig. 3A a dark-light induction of photosynthesis is presented together with Chl fluorescence recordings. In the beginning of induction both, F and F_m decreased rapidly due to the development of NPQ, so that the quenched F_m established already at 18 s past turning the light on. CEF_{II} rate was calculated as difference between the PSII charge separation rate and PSII LEF rate from O_2 evolution (Eq. (2)). Excitation partitioning a_{II} was taken 0.4 (Fig. 3A inset), assuming a constant fraction of excitation (about 20%) was quenched by charge recombination on the donor side [35]. CEF_{II} was fast in the beginning of induction – while NPQ was developing – and smoothly decreased to a minimum at the maximum ETR and during the oscillatory trough. The CEF_{II} rate significantly increased, reaching another maximum while photosynthesis was recovering from over-reduction. The amplitude of these CEF_{II} changes was 30 μmol e^- m^{-2} s^{-1} or about 15% of LEF during the recovery period.

3.2.2. Oscillations

Oscillations in photosynthesis, generated by a sudden increase of CO_2 concentration to saturating values, have been an enigma for a half

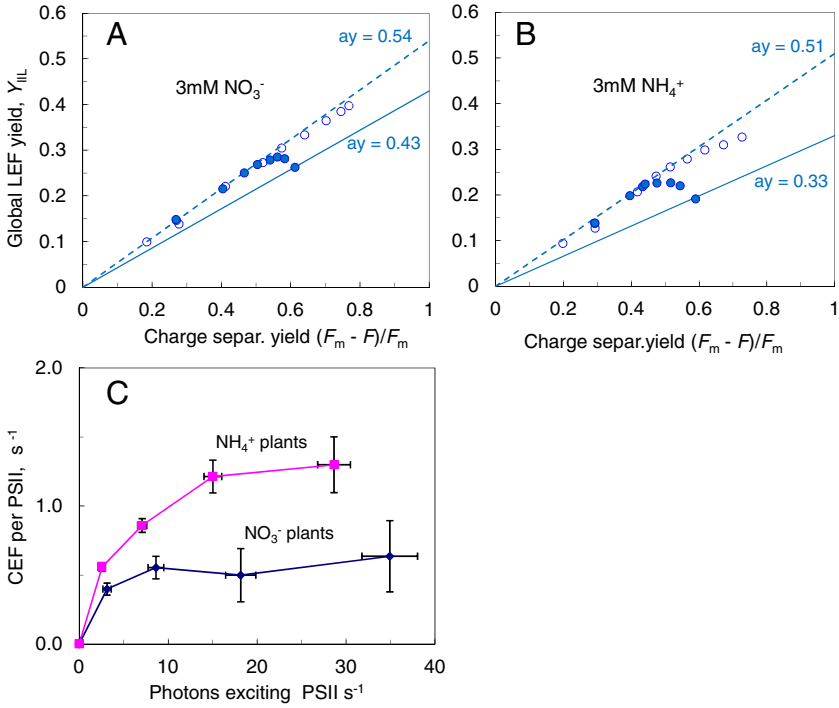

Fig. 2. Yield plots constructed from light response curves measured as in Fig. 1, except that instead of CO_2 uptake, O_2 evolution was measured in N_2 containing 20 ppm O_2 and 300 ppm CO_2. Sunflower plants were grown aeroponically with 3 mM NO_3^- (A) or 3 mM NH_4^+ (B). Panel C shows absolute rates of CEF per PSII, s^{-1}, in response to photons exciting PSII, s^{-1}. Standard errors due to biological scattering (n = 8) are indicated.

of a century. "To understand oscillations is to understand photosynthesis", stated David Walker [57]. Oscillations were initiated in O_2 evolution as shown in Fig. 3B. As soon as CO_2 concentration was increased, O_2 evolution rate rapidly increased and after 30 s reached the maximum that was more than double the previous rate at the low CO_2 concentration. However, the fast rate was not stable, but collapsed soon, approaching the bottom at about 20 s past the maximum. Chl fluorescence approached a minimum simultaneously with the maximum in O_2 evolution and reached the maximum during the collapse of O_2 evolution — an expected relationship between photochemical quenching and electron transport. Dual-intensity saturation pulses were applied periodically and the true F_m was extrapolated, which only slightly varied during the oscillations. The rate of CEF_{II} decreased during the initial fast O_2 evolution peak, but began to increase when O_2 evolution approached the collapse, reaching the maximum during the fastest increase of photosynthesis after the collapse. Such phase shift between CEF_{II} and LEF is consistent with the notion that faster PSII cycle supported the extra ATP synthesis necessary for the electron transport chain to recover from over-reduction. In twelve leaves the maximum CEF_{II} rate during the fastest recovery from the minimum was 40 ± 10 μmol m^{-2} s^{-1}, the initial maximum LEF rate was 230 ± 20 μmol m^{-2} s^{-1}.

3.3. Temporal kinetics resolve a_{II} and y_{IIL} in the ay-product

In this section we show that ± FRL treatments induced changes in CEF_{II}, but not in excitation partitioning a_{II}. The − FRL data points were measured turning FRL off for 40 s and then on again. Fig. 4 demonstrates dynamics of PSII charge separation and electron transport after FRL was turned off. The initial drop at time zero was caused by the cessation of PSII excitation by FRL, subsequent changes were caused by the accumulation of PQH_2. PSII charge separation rate (from Chl fluorescence) decreased, faster in the beginning, but the process slowed down to the end of the 40 s exposure without FRL. The rate of PSII linear electron flow (from O_2 evolution) paralleled the charge separation rate for the initial 2–3 s, but then declined. The rate of CEF_{II} – which is the difference between CSR_{II} and LEF – approached the maximum after about 30 s of the − FRL exposure.

In order to be sure that the above statement was not caused by misinterpretation of the PSII antenna drift due to state transitions, we compared temporal changes of F_m with those of the *ay* product. Under conditions where non-photochemical quenching does not change, F_m is proportional to the part of photons absorbed by PSII, a_{II}. This experiment showed that the ± FRL-induced state transition-caused changes in a_{II} were ± 11% of the total fluorescing PSII antenna and they required more than 15 min to be completed (Fig. 5). Thus, faster changes in the *ay* product were caused by y_{IIL}, i.e., by variable CEF_{II}.

3.4. Plastoquinol oxidation by dioxygen

Plastoquinol is oxidized by dioxygen enzymatically by PTOX and non-enzymatically by superoxide accumulated in the light within the membrane. In order to consider the potential interaction of both these O_2-consuming processes with our measurements we measured O_2 response curves of plastoquinol oxidation in sunflower leaves using Chl fluorescence as an indicator of the PQH_2 level.

A leaf was pre-adapted in darkness for 15 min in 21% O_2, in order to inactivate FNR. Then the required O_2 concentration was set, a fluorescence-saturation pulse was applied and the time courses of fluorescence induction during the pulse and fluorescence yield decay after the pulse were recorded (Fig. 6). After the pulse, variable fluorescence within 2–3 s decreased to the level of 0.2 ± 0.01 F_v (which we term "residual fluorescence", F_r), but its further decay from F_r to F_0 was strongly dependent on O_2 concentration. At 20 ppm O_2 fluorescence remained at the F_r level, but at higher O_2 concentrations it decreased exponentially, approaching F_0 the faster the higher was O_2 concentration (Fig. 7). The rate constant of $F_r \rightarrow F_0$ fluorescence decay depended on the O_2 concentration in accordance with a rectangular hyperbola with the half-saturation concentration $K_m(O_2)$ of 60 μM or 4.6% O_2 in the gas phase (Fig. 8).

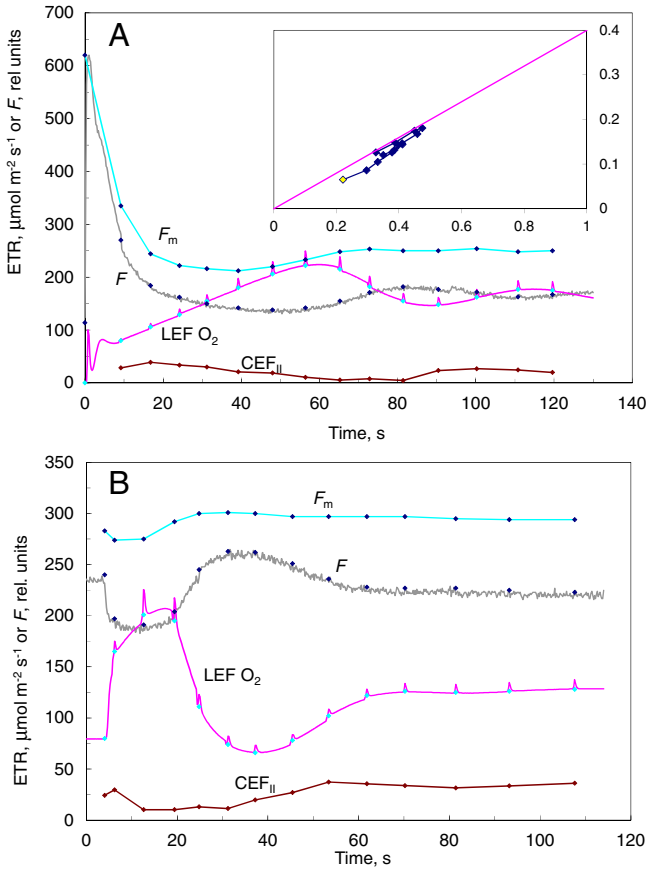

Fig. 3. Fast CEF_{II} during recovery from over-reduction. Panel A: Dark-light induction of photosynthesis. A sunflower leaf was dark-adapted for 15 min and light (630 nm, PAD = 1226 μmol m^{-2} s^{-1}) was turned on at time = 0. Fluorescence F was recorded and F_m was measured when indicated by spikes in O_2 evolution. CEF_{II} was calculated as difference between CSR_{II} (Eq. (4), a_{II} = 0.40 see inset) and LEF (Eq. (2)). Panel B: Oscillations in photosynthesis. CO_2 concentration was increased from 200 to 2000 ppm at time = 5 s, PAD = 1226 μmol m^{-2} s^{-1}. Denotations as in panel A.

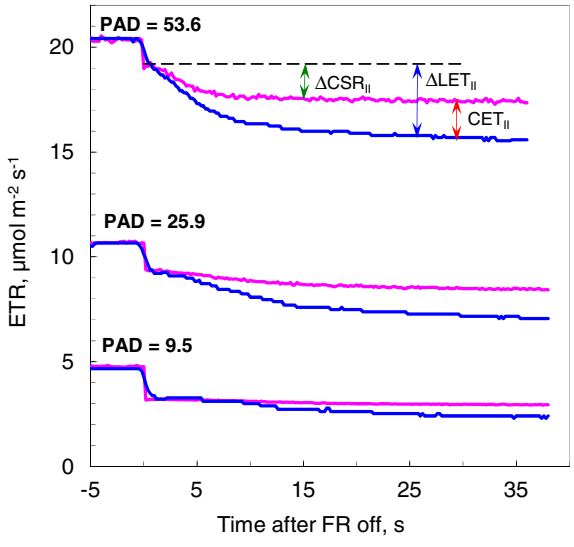

Fig. 4. Time courses of CSR_{II} (red) and LEF (blue) after far-red light was turned off at time = 0. Arrows indicate changes in PSII charge separation rate indicated by fluorescence increase, ΔCSR_{II}, in linear electron flow through PSII, ΔLEF_{II}, and cyclic electron flow through PSII, CEF_{II}. Absorbed PAD (630 nm + FRL exciting PSII) is indicated at the curves.

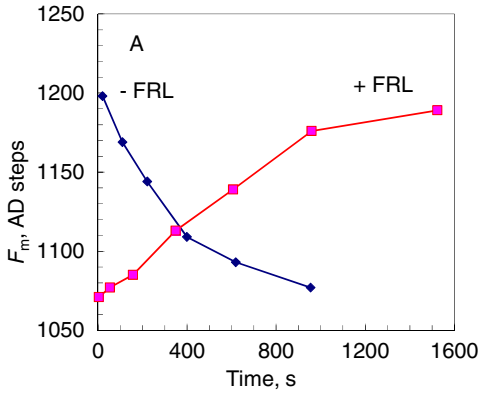

Fig. 5. Changes in F_m caused by state transitions induced by turning FRL off and on. Photosynthesis was stabilized at 45.4 μmol e^- m^{-2} s^{-1}, 647 nm AL + FRL of 20 μmol m^{-2} s^{-1}, then FRL was turned off and F_m was repeatedly measured (blue line). After 1000 s FRL was turned on and F_m was measured again (red line). Ordinate is given in steps of the A/D converter. F_m was measured by extrapolation using dual-intensity saturation pulses, 7000 μmol m^{-2} s^{-1} for 300 ms and 3500 for 200 ms.

In the above analysis critical was the point that the initial fast drop of fluorescence from the F_m to the F_r level was not accompanied by significant oxidation of PQH_2, but the latter became oxidized during the slow process accompanied by fluorescence decrease from F_r to F_0. In order to relate fluorescence level to the PQH_2 pool size we repeated the induction after different dark intervals, measuring the complementary area [35]. These measurements were carried out at 21% O_2, considering that PQH_2 is oxidized even more slowly at lower O_2 concentrations. Though the total complementary area increased rather rapidly with prolonging the dark interval between the inductions, it initially reflected electron flow away from the acceptor side of PSI due to the activation of FNR by the first pulse (Fig. 9A). The reduction level of PQ was best reflected by the fast initial increase of fluorescence, which reached the level of >0.9 F_m by the transport of only 1 μmol e^- m^{-2} (Fig. 9B). In the CSR_{II} presentation of Fig. 9A F_m corresponds to zero CSR_{II} and the initial peak of fluorescence corresponds to the deep minimum of CSR_{II}. The progress of this minimum (or the fluorescence maximum in Fig. 9B) with the delay time shows the reduction level of PQ had barely changed during the initial 3 s of darkness, during which fluorescence had already dropped to the F_r level. In the presence of 21% O_2 plastoquinol became mostly oxidized after dark intervals of

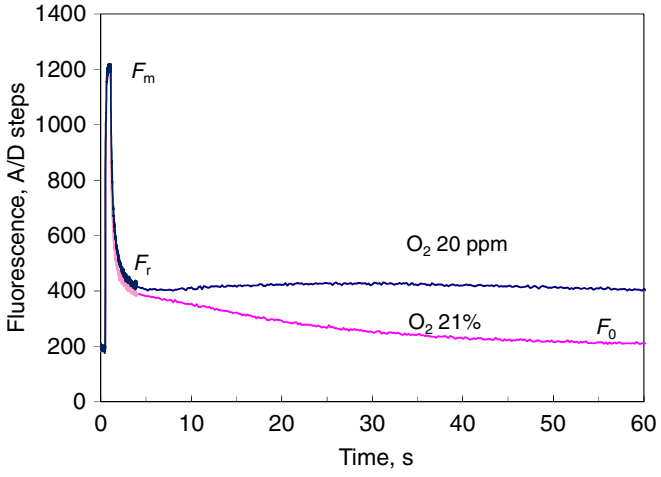

Fig. 6. Time course of fluorescence yield changes during a saturation pulse (F_m), followed by decay in the dark at 20 ppm and 21% O_2.

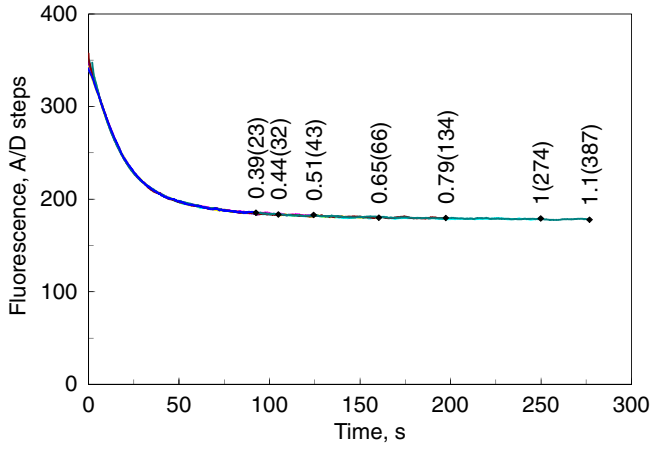

Fig. 7. Dark decay of fluorescence yield at different O_2 concentrations. Time = 0 was set to 2.9 s past the saturation pulse and the dark decay of fluorescence was recorded during 250 s at different O_2 concentrations. The curve at 274 μM O_2 (21%) was plotted against time as recorded. For other O_2 concentrations (indicated in parentheses, μM) time was multiplied by the factor standing in front of the parentheses (e.g. 1.0 for 274 and 0.51 for 43 μM O_2). As a result of this the end of the recording (250 s) shifted as indicated by a highlighted data point on the curve. Data on ordinate are as recorded, not normalized. The fluorescence decay curve is an exponential with rate constant of 0.054 s^{-1} for 274 μM O_2. At other O_2 concentrations the rate constant was smaller or bigger by the factor indicated in front of the parentheses.

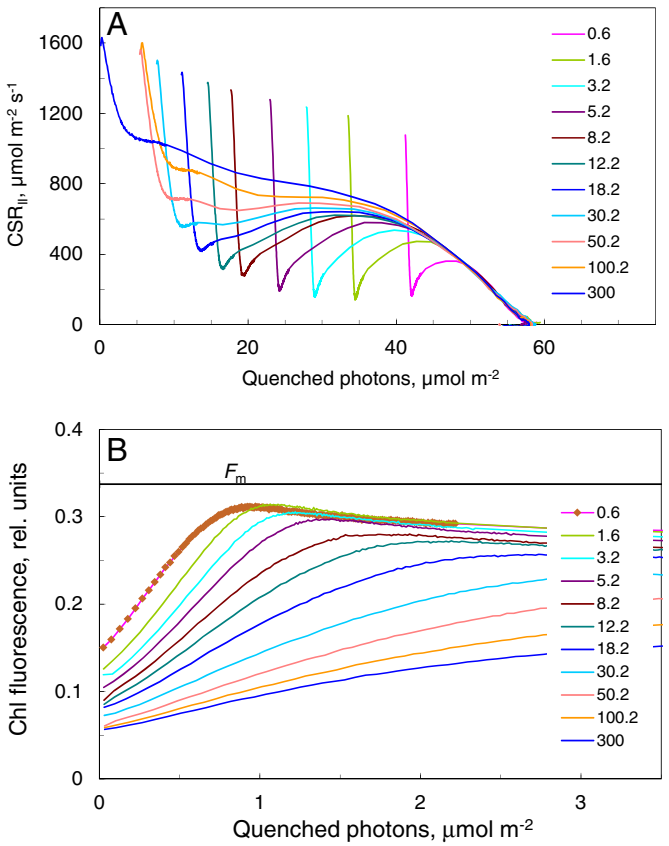

Fig. 9. Complementary area analysis of fluorescence induction. A dark-adapted leaf was illuminated by a saturation pulse reducing the whole electron transport chain. After a dark time as listed in the legend (seconds) another saturation pulse was applied, for which fluorescence induction was recorded. Cumulative complementary area (doze of photochemically quenched photons, μmol m^{-2}) was calculated and plotted on the abscissa (see also [35]). On panel A PSII charge separation rate CSR_{II} (Eq. (4), $a_{II} = 0.58$) is plotted against quenched photons. On panel B the initial parts of the fluorescence induction curves are plotted against quenched photons (individual sampled data points are shown for one curve).

longer than 30–50 s, as indicated by initial fluorescence in the beginning of induction.

Thus, whatever the mechanism of the adjustment of F_r (see Discussion), the kinetics of fluorescence decrease from F_r to F_0 are related to the gradual oxidation of the initially nearly fully reduced PQH_2 pool to the finally mostly oxidized PQ pool. The exponential shape of the fluorescence decay curve suggests that fluorescence level between F_0 and F_r is proportional to plastoquinone reduction state, i.e., PQH_2 oxidation by dioxygen is a first-order reaction in relation to PQH_2 concentration. Kinetics of PQH_2 oxidation in response to O_2 concentration (Fig. 8) are closely represented by a Michaelis–Menten type hyperbola with $K_m(O_2)$ of 60 μM (4.6% in the gas phase).

3.5. Oxygen was not an electron acceptor for PQH_2 oxidation

A theoretical possibility remains that oxygen produced by PSII during photosynthesis increases local concentration in thylakoids to the level that O_2 still reacts with PQH_2. This phenomenon would be similar to the local decrease of CO_2 concentration in chloroplasts caused by binding of CO_2 to ribulose 1,5-bisphosphate, which, at fast rates extends to several hundreds of ppm. Leaf diffusion resistances in the gas phase were routinely measured together with the O_2 evolution flux. Mesophyll diffusion resistance in the liquid phase, r_l, was derived for every individual leaf (see Materials and methods). Average values for the 16 leaves of the experiments of Fig. 2 were $r_g = 0.214 \pm 0.014$ and $r_l = 0.01 \pm 0.0006$ s mm^{-1} for O_2. Oxygen concentration in chloroplast, O_C, was calculated for PAD of 35 μmol m^{-2} s^{-1} for every leaf, resulting in the average value of $O_C = 0.068 \pm 0.002$ μM during photosynthesis at 35 μmol quanta m^{-2} s^{-1} (for comparison, at saturating light O_C was 0.51 ± 0.03 μM). This O_2 concentration was low enough to avoid PQH_2 oxidation interfering with the PSII cycle.

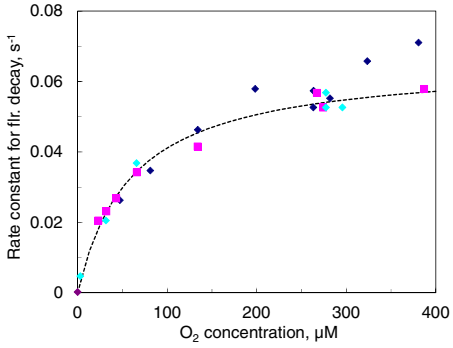

Fig. 8. Oxygen concentration dependence of the first-order rate constant of the slow-phase fluorescence yield decay, determined as shown in Fig. 7.

4. Discussion

4.1. Proton transporting PSII cycle

Cyclic electron flow around PSII is known, but so far it seldom has been related to proton transport and ATP synthesis. As in the PSI cycle [58], there is a fast component in the PSII cycle that evidently is not proton-coupled, but facilitates charge recombination within PSII at high light intensities [33]. Parallel measurements revealed that the higher the light intensity, the larger became the gap between the rate of PSII charge separation as detected from Chl fluorescence and the rate of LEF through PSII as detected from O_2 evolution [34,51]. The difference was explained by charge recombination on the donor side of PSII, from excited P680* to oxidized tyrosine Z [35]. This mechanism

participates in experiments carried out at high PADs in this work. For example, the saturating-light data points in our yield plots (Figs. 1, 3) indicated reduced a_{II} values, caused by the donor side charge recombination. The rate of this fast PSII cycle decreased, but contrary to expectations did not disappear at limiting light intensities [34], suggesting the presence of another type of CEF_{II} — a slow component not related to charge recombination.

In the present work we showed that the slow CEF_{II} depended on excitation balance between the photosystems. Varying excitation partitioning between the two photosystems in a sunflower leaf we found that as soon as PQH_2 accumulated due to PSII over-excitation, CO_2 uptake and O_2 evolution decreased more than that was accountable by the increased Q_A reduction. The so detected PSII cycle was running faster under conditions requiring more extra ATP, such as the absence of nitrite as an alternative electron acceptor and severe over-reduction of electron transport chain during induction and oscillations of photosynthesis, suggesting that this PSII cycle is supporting ATP synthesis.

The PSII cycle supporting ATP synthesis has been reported only in one paper. Daniel Arnon and George Tsang wrote [59]: "This paper reports evidence and outlines a hypothesis in support of a "b-559 cycle" — i.e., a light-induced, cytochrome b-559-dependent, cyclic electron transport around PSII that promotes translocation of protons from plastoquinol into the aqueous domain (lumen) of photosynthetic membranes (thylakoids)." These authors were guided by analogy between the Cyt b_6f complex and PSII, both containing hemes. Their experimental evidence was based on favored photo-oxidation of Cyt b_{559} in the presence of proton uncouplers and protonofores, suggesting that the cycle is controlled by the counter-pressure of protons. The proposed mechanism of oxidation of a PQH_2 molecule by sharing electrons between Cyt b_{559} (PSII) and the Rieske FeS center (Cyt b_6f complex) however was unrealistic, therefore the paper was forgotten.

In this work we re-incarnate the idea of [59]. Our kinetic evidence that the PSII cycle is running faster under conditions requiring additional ATP synthesis strongly suggests that the plastoquinol-oxidizing PSII cycle is coupled with vectorial proton transfer. The oxidation of PQH_2 is inevitably coupled with proton release anyway, therefore, the question may be only, is the transport transmembrane? The presence of two quinone binding sites in one protein complex is a prerequisite for the Q-cycle type proton transport, where protons are bound to the PQ being reduced at one side and are released from the PQH_2 being oxidized at the other side of the membrane. Another quinol binding site, Q_C, different from Q_B, was postulated to be responsible for the redox potential changes of Cyt b_{559} [29,60,61]. The Q_C site was identified in cyanobacterial PSII [62]. Nevertheless, the more recent X-ray structure at 1.9 Å resolution [63] did not show Q_C, casting doubt on the existence of the Q_C binding site, or at least showing that its detection depends on the conditions of sample preparation — as expected if this quinone participates in the cyclic electron transport.

Based on the potential presence of the two quinone binding sites in the PSII complex we propose the following putative mechanism for the proton transfer-coupled reduction–oxidation of plastoquinone by PSII. The reducing/protonating site is the Q_B site near the stroma, but the oxidizing/deprotonating site is Q_C. According to Guskov et al. [62], in Q_C the quinol resides with a portal between PsbJ and Cyt b_{559} and forms van der Waals contacts with Car_{D2} and the phytol chain of Chl_{D2}, also with some fatty acids and the isoprenoid chain of Q_B, but not with the protein. Its head group is 17 Å away from the head group of Q_B and 15 Å from the heme of Cyt b_{559} (edge-to-edge distances), in agreement with indirect evidence suggesting the presence of a PQ binding site near Cyt b_{559} [64]. The fact that CEF_{II} generally did not run in the + FRL measurements shows that the Q_O site of Cyt b_6f is a stronger competitor for PQH_2 than the Q_C site of PSII, which has relatively low affinity to the substrate [65].

We propose the following scenario of electron transfers. After a PSII excitation an electron is transferred from P680 to Q_A (Fig. 10, step 1). A plastoquinol bound at the Q_C site is oxidized faster than Tyr Z (within 1 μs), donating one electron to $P680^+$ via Car_{D2} and Chl_{D2} (as described in Introduction), but simultaneously the other electron moves to Cyt b_{559} (step 2). On the PSII acceptor side the electron moves from Q_A to Q_B (several hundreds μs). The formed semiquinone radical Q_B^- is a strong oxidant, attracting an electron from Cyt b_{559} to form the stable PQH_2 molecule (step 3).

The novelty of this scheme is electron transfer in the direction opposite to that commonly assumed – from reduced Cyt b_{559} to Q_B^-. Though the distance between Q_B and Cyt b_{559} is 25 Å [62], electron transfer from Q_B to Cyt b_{559} has been considered possible [40,66]. Therefore, as well possible could be the reduction of Q_B^- by electron transfer from Cyt b_{559}, either directly or making use of the semiquinone transfer orbital on the still Q_C–bound PQ, which would shorten the jumping distances to 17 and 15 Å [62]. If such a PSII cycle could function at its full rate, a plastoquinol would be fully oxidized and another one reduced with a single electron transfer through PSII according to the scenario of Fig. 10. The key of this scheme is the competitive electron transfer to $P680^+$ either from Y_Z or from Car_{D2}. Though donation by Y_Z is fast [67], the carotenoid still seems to be a successfully competing reductant, as proven by numerous examples of photo-oxidation of pre-reduced Cyt b_{559}. The major problem of this model is the placement of the Q_C site, which is not close to the lumenal side of the membrane, but is situated

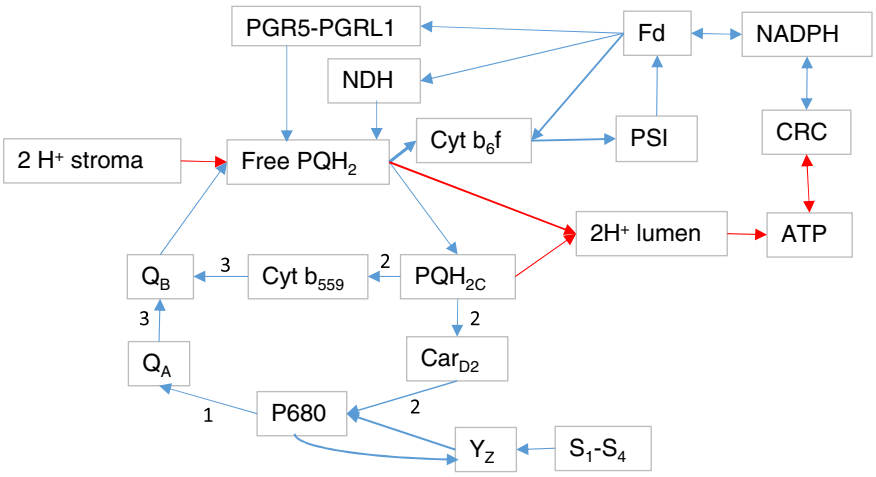

Fig. 10. Putative mechanism of the PSII cycle (reactions 1, 2, 3) and the cooperating (complementary) plastoquinol-centered cyclic electron transport pathways.

rather deeply in the membrane. Nevertheless, protons may be transferred along special channels, as it happens during Q_B protonation and water oxidation.

In summary, there is enough evidence about circumstances where the photosynthetic linear electron flow alone cannot support ATP synthesis at the rate compatible with the rate of NADPH synthesis. Several complementary electron transport processes serve to compensate for the ATP deficit, such as linear flow to alternative acceptors other than carbon reduction and cycling of electrons, forcing them to pass through the proton-coupled step again. So far only one proton-coupled electron transfer process was known in photosynthesis – the Q-cycle in the cytochrome b_6f complex – contrary to several proton-coupled electron transfer loops inside complexes I, III and IV of the respiratory electron transport chain. In this work we bring evidence about the existence of another Q-cycle type process in photosynthesis — the Q-cycling of electrons inside PSII, oxidizing and reducing diffusible plastoquinone.

The PSII Q-cycle becomes activated under conditions where additional ATP is needed and PSII is sufficiently over-excited compared to PSI. Being directly related to the plastoquinone reduction level, it can explain why non-photochemical quenching of PSII fluorescence is correlated with Q_A reduction, and why plastoquinone reduction level signals about state 2 → state 1 transition [68]: participating in vectorial proton transfer plastoquinol supports additional ATP synthesis, necessary for phosphorylation of the movable LHCII units. The PSII cycle is responsible for the frequently observed decreased quantum yield of photosynthesis under stress conditions and for "misses" in the period-four advancement of the S-states [69]. Possibly, just the more active PSII cycle could ensure the growth of the *Chlamydomonas* mutant with inactivated redox loop of the Q-cycle [70], consistent with the notion that numerous proton-coupled cyclic and pseudocyclic processes are mutually complementary.

4.2. Plastoquinol oxidation by dioxygen

The existence of the PSII cycle was deduced from kinetic responses of O_2 evolution and Chl fluorescence to changes in excitation partitioning between PSII and PSI. As typical to kinetic analysis, similar responses could be caused by different internal processes. Therefore, in our experiments care was taken to eliminate competing processes, potentially biasing the conclusions.

The decrease in PSII linear electron flow in response to the accumulation of PQH_2 was not caused by changes in the antenna size, as the effect was fast (within 30 s, Fig. 4). Contrary to this, the state 1–state 2 transition required 15 min to be completed (Fig. 5). The amplitude of the state transition-caused F_m changes was 11%, indicating that one "loosely bound" L type LHCII trimer (42 Chls) was moved per every $C_2S_2M_2L_2$ PSII dimer (376 Chls). This is in general agreement, though somewhat less than reported in [71], probably because our experimental conditions did not induce a full-size state-transition.

Oxidation of PQH_2 by dioxygen could be a competitor process to the oxidation of PQH_2 by PSII (see Introduction). In order to carefully eliminate this possibility we measured the concentration dependence of the rate of PQH_2 oxidation by oxygen and showed that under our experimental conditions PQH_2 oxidation by O_2 was by at least two orders of magnitude slower than the measured rate of PQH_2 oxidation.

We used Chl fluorescence to indicate the reduction level of PQ. Fluorescence approached F_m and PQ became nearly fully reduced to the end of the 0.6 s dark-light induction under the high PFD of 4000 μmol m^{-2} s^{-1}. After the actinic light was turned off, within three seconds fluorescence dropped from the F_m level to an intermediate F_r level at about 0.2 F_v. The rate of this fluorescence drop was faster at higher O_2 concentrations, but the F_r level was the same independent of the presence or absence of oxygen. Further decrease of fluorescence from F_r to F_0 was much slower, the rate clearly depending on O_2 concentration. In this range the rate of fluorescence decrease was proportional to $F - F_0$, indicating that the substance causing the rise of F over F_0 was decreasing with the rate proportional to its own level, i.e., obeying first-order kinetics. The rate-constant of this first-order decay was 0.054 s^{-1} at 270 μmol O_2 (21%). It depended on O_2 concentration, obeying approximately hyperbolic kinetic curve with $K_m(O_2)$ of 60 μM in liquid phase (4.6% in gas phase).

The reduction state of Q_A determines fluorescence level between F_0 and F_m either nonlinearly due to excitonic connectivity [72] or linearly, as detected in experiments where Q_A reduction was induced by gradual acceptor side closure [35,73]. Therefore, the initial fast drop of fluorescence in the dark immediately after the induction was certainly caused by Q_A oxidation in a part of the PSII-s. A competing electron acceptor for this process was O_2, but fluorescence dropped from F_m to F_r in the absence of O_2 as well. A potential pathway for Q_A oxidation could be reversal of the non-photochemical Q_A reduction pathway, usually related to plastid NAD(P)H:plastoquinone oxidoreduction complex or to the PROTON GRADIENT REGULATION PGR5/PGRL1:plastoquinone reductase, but recently shown to be directly linked with Q_A reduction [14]. Assuming this process, Q_A rapidly dropped to a level equilibrated with the non-photochemically reducing substrates, mainly NADPH and reduced Fd, and the further slow decrease of fluorescence could be caused by the oxidation of these non-photochemical reducers, not by the oxidation of PQH_2. Contrary to this, our complementary area measurements showed that PQH_2 indeed was oxidized during the secondary slow phase of fluorescence decrease. Importantly, in different experiments the F_r level was rather constantly 0.2 ± 0.01 F_v (Fig. 7), suggesting that the F_r level was determined by rather stable factors or relationships. We suggest that the dominant electron transfer process, causing the initial rapid Q_A oxidation, was charge recombination from Q_A^- to the S-states, accompanied by electron transfer to O_2 when this oxidant was present. The state with fully reduced PQ is analogous to the DCMU-inhibited state of PSII. Thus, the initial fast phase of fluorescence yield decay corresponds to the fluorescence yield decay after initial flash reduction in DCMU-treated objects, which also occurs within 1–2 s [69]. This hypothesis is consistent with the F_r level of close to 1/4 F_v, indicating that charge recombination was impossible into one of the four stable S-states — probably the one that just had performed O_2 evolution. Reasons why F_r actually was <1/4 F_v could be incomplete randomization of the S-states to the end of the 0.6 s induction process and excitonic connectivity between the PSII antennae.

According to this model, fluorescence remained at the F_m level in approximately one fourth of the PSII units, dropping to F_0 after PQH_2 was replaced by PQ in their Q_B site, making electron transfer from Q_A to Q_B possible. This model is well consistent with the measurements showing that PQ remained highly reduced, though fluorescence decreased from F_m to the F_r level. Plastoquinone was oxidized during the slow phase, being reflected by fluorescence decrease from F_r to F_0. Our dual phase decrease of fluorescence is also consistent with the dual phase oxidation of quinone as detected spectrophotometrically by ΔA_{263} [74] — in the cited work the fast phase could be Q_A oxidation, but only the slow phase was PQH_2 oxidation. This may question the conclusion of the last-cited work that the dual phase process could not be PTOX-based enzymatic oxidation of PQH_2, but was mainly non-enzymatic oxidation initiated by O_2^-.

As mentioned above, interdependence between Chl fluorescence and PQ reduction level is generally considered to be nonlinear, first because of the redox potential difference between plastoquinol and the Q_A semiquinone and, second, because of excitonic connectivity between PSII antennae. Contrary to this, our experiments showed precise first-order characteristics with respect to Chl fluorescence: the rate of fluorescence yield decay was proportional to the level of fluorescence between F_r and F_0 — at all O_2 concentrations fluorescence quenched exponentially from F_r to F_0 (Fig. 7). It would be difficult to explain such a linearity on the basis of occasional overlapping of several nonlinearities having opposite direction. Rather we tend to believe that during the decay from F_r to F_0 fluorescence proportionally reflected the

PQH_2 level, consistently with PQH_2 being a strongly binding competitive product inhibitor for PSII [51]. Thus, we interpret our experiments showing that the kinetics of PQH_2 oxidation are of the first order with respect to PQH_2 concentration over its full redox range; with respect to O_2 the kinetics saturate with an apparent $K_m(O_2)$ of 60 μM (4.6%). The latter parameter is in agreement with the nature of the PTOX enzyme, belonging to the family of alternative oxidases having relatively low affinity to oxygen with $K_m(O_2)$ of 10–20 μM [75]. But rather unexpected is the first-order kinetics with respect to the PQH_2 pool. Knowing that there are about 3 PQH_2 per PSII and only one PTOX per 100 PSII [20,21], we get about 300 PQH_2 molecules per one PTOX enzyme. Nevertheless the reaction is first-order with respect to PQH_2, which indicates a very low binding constant of PQH_2 to the enzyme, or still supports the non-enzymatic mechanism of the reaction [74].

In order to evaluate the rate of PQH_2 oxidation by O_2 in comparison with the PQH_2 oxidizing PSII cycle we proceed from the total pool size of 3 PQH_2 per PSII in sunflower [51] and PSII density of 1.6 μmol m^{-2}, resulting in 9.6 μmol e^- m^{-2} in the fully reduced PQH_2 pool. Using the fluorescence decay rate constant of 0.054 s^{-1} at 21% O_2 (Fig. 8) we obtain the maximum rate of PQH_2 oxidation of 0.52 μmol e^- m^{-2} s^{-1} or 0.32 e^- s^{-1} per PSII, which is in good agreement with the evaluation "smaller than 1 electron per second per PSII" [24], making up about one third of the recorded CEF_{II} rate (Fig. 2C). However, this estimated rate corresponds to 270 μM (21%) O_2 and fully reduced PQH_2. Under our experimental conditions of Fig. 2, where the typical intrachloroplast O_2 concentration generated by the photosynthetic O_2 evolution $O_C = 0.068 \pm 0.002$ μM and PQ was only a little reduced, the rate of PQH_2 oxidation was undetectably slow. Thus, in our low-O_2 experiments the potential rate of oxidation of PQH_2 by dioxygen was by at least two orders of magnitude slower than the detected rate of PQH_2 oxidation by PSII.

Our calculations of the chloroplast O_2 concentration (Section 3.5.) were carried out on an assumption that the diffusion pathways were similar for CO_2 and O_2. Indeed, no specific barriers are known for O_2 diffusion in cells that could cause extraordinary accumulation of this dissolved gas in chloroplasts. Nevertheless, sometimes kinetic phenomena have been interpreted showing preferably direct re-assimilation of photosynthetically generated oxygen. In a related report [76] green alga *Chlorella sorokiniana* were suspended in oxygen-free aqueous medium, due to which the respiratory electron transport chain became reduced. When the suspension was illuminated with saturating ST flashes, partial oxidation of electron carriers was recorded typically within about 3 ms, followed by re-reduction within 20 ms. It was estimated that about 30% of the photosynthetic oxygen could be directly re-assimilated by mitochondria via an intracellular transport pathway. Temporal kinetics of the diffusion process were estimated, showing that in homogeneous medium at 3 ms an oxygen molecule is typically found at the distance of 3.5 μm away from its origin. Because the cells of *C. sorokiniana* have a diameter of 2 μm [76], this means that at 3 ms the photosynthetically evolved oxygen was about equally distributed over the whole cell, without any diffusion restrictions inside cells.

Thus, reassimilation of photosynthetically evolved oxygen indeed occurs in algal cells suspended in aqueous medium, the latter forming the necessary diffusion barrier at the cell surface. The treatments used in the cited work involved an extraordinarily strong O_2 evolution pulse of 0.58 O_2 molecule per PSII center, which was far lower in our experiments, especially in those carried out at low light. The O_2 detection system used in the cited work – the mitochondrial terminal cytochrome oxidase – was far more sensitive to O_2 ($K_m(O_2) = 190$ ppm [77]), contrary to PTOX ($K_m(O_2) = 4\%$), in focus in this work. And, most important, in leaves at cell walls O_2 concentration equals to the gaseous concentration, while in algae water forms a continuous strong diffusion barrier. Therefore, our assumption that the diffusion pathways were similar for CO_2 and O_2, not involving any specific intracellular diffusion channels, was correct. The photosynthetically evolved oxygen in no way could oxidize plastoquinol at a rate comparable to the rate of the PSII cycle.

Transparency Document

The Transparency document associated with this article can be found, in the online version.

Acknowledgment

This work was supported by personal grant 0393P from Ministry of Education and Science, Estonia.

References

[1] K.E. Wilson, A.G. Ivanov, G. Öquist, B. Grodzinski, F. Sarhan, N.P.A. Hüner, Energy balance, organellar redox status and acclimation to environmental stress, Can. J. Bot. 84 (2006) 1355–1370.
[2] P.G. Falkowski, Y.B. Chen, Photoacclimation of light harvesting systems in eukatyotic algae, in: B.R. Green, W.W. Parsons (Eds.), Light harvesting antennas in photosynthesis, Kluwer Academic Publishers, Dordrecht, The Netherlands, 2003, pp. 423–447.
[3] J.M. Escoubas, M. Lomas, J. LaRoche, P.G. Falkowski, Light intensity regulation of cab gene transcription is signaled by the redox state of the plastoquinone pool, Proc. Natl. Acad. Sci. U. S. A. 92 (1995) 10237–10241.
[4] B. Ivanov, M. Kozuleva, M. Mubarakshina, Oxygen metabolism in chloroplast, in: P. Bubulya (Ed.), Cell Metabolism — Cell Homeostasis and Stress Response, In-Tech, Rijeka, Croatia, 2012.
[5] H. Seelert, N.A. Dencher, D.J. Müller, Fourteen protomers compose the oligomer II of the proton-rotor in spinach chloroplast ATP synthase, J. Mol. Biol. 333 (2003) 337–344.
[6] L.A. Sazanov, P. Burrows, P.J. Nixon, Presence of a Large Protein Complex Containing the *ndh*K Gene Product and Possessing NADH-specific Dehydrogenase Activity in Thylakoid Membranes of Higher Plant Chloroplasts, Kluwer Academic Publishers, Dordrecht, the Netherlands, 1995.
[7] H. Jamamoto, L. Peng, Y. Fukao, T. Shikanai, An Src homology 3 domain-like fold protein forms a ferredoxin binding site for the chloroplast NADH dehydrogenase-like complex in *Arabidopsis*, Plant Cell 23 (2011) 1480–1493.
[8] T. Joët, L. Cournac, E.M. Horvath, P. Medgyesy, G. Peltier, Increased sensitivity of photosynthesis to antimycin A induced by inactivation of the chloroplast *ndhB* gene. Evidence for a participation of the NADH-dehydrogenase complex to cyclic electron flow around photosystem I, Plant Physiol. 125 (2001) 1919–1929.
[9] Y. Munekage, M. Hojo, J. Meurer, T. Endo, M. Tasaka, T. Shikanai, PGR5 is involved in cyclic electron flow around photosystem I and is essential for photoprotection in *Arabidopsis*, Cell 110 (2002) 361–371.
[10] Y. Munekage, M. Hashimoto, C. Miyake, K.-I. Tomizawa, T. Endo, M. Tasaka, T. Shikanai, Cyclic electron flow around photosystem I is essential for photosynthesis, Nature 429 (2004) 579–582.
[11] G. DalCorso, P. Pesaresi, S. Masiero, E. Aseeva, D. Schünemann, G. Finazzi, P. Joliot, R. Barbato, D. Leister, A complex containing PGRL1 and PGR5 is involved in the switch between linear and cyclic electron flow in *Arabidopsis*, Cell 132 (2008) 273–285.
[12] A.P. Hertle, T. Blunder, T. Wunder, P. Pesaresi, M. Pribil, U. Armbruster, D. Leister, PGRL1 is the elusive ferredoxin–plastoquinone reductase in photosynthetic cyclic electron flow, Mol. Cell 49 (2013) 511–523.
[13] D. Leister, T. Shikanai, Complexities and protein complexes in the antimycin A-sensitive pathway of cyclic electron flow in plants, Front. Plant Sci. 4 (2013) 1–4, http://dx.doi.org/10.3389/fpls.2013.00161.
[14] N. Fisher, D.M. Kramer, Non-photochemical reduction of thylakoid photosynthetic redox carriers in vitro: relevance to cyclic electron flow around photosystem I? Biochim. Biophys. Acta 1837 (2014) 1944–1954.
[15] P. Gans, F. Rebeille, Control in the dark of the plastoquinone redox state by mitochondrial activity in *Chlamydomonas reinhardtii*, Biochim. Biophys. Acta 1015 (1990) 150–155.
[16] P. Carol, D. Stevenson, C. Bisanz, J. Breitenbach, G. Sandmann, et al., Mutations in the *Arabidopsis* gene *immutans* cause a variegated phenotype by inactivating a chloroplast terminal oxidase associated with phytoene desaturation, Plant Cell 11 (1999) 57–68.
[17] D.Y. Wu, D.A. Wright, C. Wetzel, D.F. Voytas, S. Rodermel, The *immutans* variegation locus of *Arabidopsis* defines a mitochondrial alternative oxidase homolog that functions during early chloroplast biogenesis, Plant Cell 11 (1999) 43–55.
[18] L. Cournac, E.M. Josse, T. Joet, D. Rumeau, K.E. Redding, et al., Flexibility in photosynthetic electron transport: a newly identified chloroplast oxidase involved in chlororespiration, Philos. Trans. R. Soc. Lond. Ser. B 355 (2000) 1447–1453.
[19] E.M. Josse, A.J. Simkin, J. Gaffe, A.M. Laboure, M. Kuntz, P. Carol, A plastid terminal oxidase associated with carotenoid desaturation during chromoplast differentiation, Plant Physiol. 123 (2000) 1427–1436.
[20] T. Joët, B. Genty, E.-M. Josse, M. Kunz, L. Cournac, G. Peltier, Involvement of a plastid terminal oxidase in plastoquinone oxidation as evidenced by expression of the *Arabidopsis thaliana* enzyme in tobacco, J. Biol. Chem. 277 (2002) 31623–31630.
[21] A.M. Lennon, P. Prommeenate, P.J. Nixon, Location, expression and orientation of the putative chlororespiratory enzymes, Ndh and IMMUTANS, in higher-plant plastids, Planta 218 (2003) 254–260.

[22] E.-M. Josse, J.-P. Alcaraz, A.-M. Laboure', M. Kunz, In vitro characterization of a plastid terminal oxidase (PTOX), Eur. J. Biochem. 270 (2003) 3787–3794.
[23] K.K. Niyogi, Safety valves for photosynthesis, Curr. Opin. Plant Biol. 3 (2000) 455–460.
[24] M. Trouillard, M. Shabazi, L. Moyet, M. Rappaport, P. Joliot, M. Kunzel, G. Finazzi, Kinetic properties and physiological role of the plastoquinone termonal oxiase (PTOX) in a vascular plant, Biochim. Biophys. Acta 1817 (2012) 2140–2148.
[25] Y. Allahverdiyeva, F. Mamedov, P. Mäenpää, I. Vass, E.-M. Aro, Modulation of photosynthetic electron transport in the absence of terminal electron acceptors: characterization of the *rbcL* deletion mutant of tobacco, Biochim. Biophys. Acta 1709 (2005) 69–83.
[26] M.M. Mubarakshina, B.N. Ivanov, The production and scavenging of reactive oxygen species in the plastoquinone pool of chloroplast thylakoid membranes, Physiol. Plant. 140 (2010) 103–110.
[27] Y. Takahashi, K. Asada, Superoxide production in aprotic interior of chloroplast thylakoids, Arch. Biochem. Biophys. 267 (1988) 714–722.
[28] J. Kruk, K. Strzalka, Dark reoxidation of the plastoquinone-pool is mediated by the low-potential form of cytochrome b-559 in spinach thylakoids, Photosynth. Res. 62 (2–3) (1999) 273–279.
[29] J. Kruk, K. Strzalka, Redox changes of cytochrome b_{559} in the presence of plastoquinones, J. Biol. Chem. 276 (2001) 86–91.
[30] U. Heber, M.R. Kirk, N.K. Boardman, Photoreductions of cytochrome b-559 and cyclic electron flow in photosystem II of intact chloroplasts, Biochim. Biophys. Acta 546 (1979) 292–306.
[31] C. Miyake, A. Yokota, Cyclic flow of electrons within PSII in thylakoid membranes, Plant Cell Physiol. 42 (2001) 508–515.
[32] P.G. Falkowski, I. Fujita, A. Lay, D. Mauzerall, Evidence for cyclic electron flow around photosystem II in *Chlorella pyrenoidasa*, Plant Physiol. 81 (1986) 310–312.
[33] A. Laisk, H. Eichelmann, V. Oja, B. Rasulov, H. Rämma, Photosystem II cycle and alternative electron flow in leaves, Plant Cell Physiol. 47 (2006) 972–983.
[34] A. Laisk, H. Eichelmann, V. Oja, Oxygen evolution and chlorophyll fluorescence from multiple turnover light pulses: charge recombination in photosystem II in sunflower leaves, Photosynth. Res. 113 (2012) 145–155.
[35] A. Laisk, V. Oja, Thermal phase and excitonic connectivity in fluorescence induction, Photosynth. Res. 117 (2013) 431–448.
[36] J. Whitmarsh, H.B. Pakrasi, Form and function of cytochrome b-559, in: D. Ort, C.F. Yocum (Eds.), Oxygenic Photosynthesis: The Light Reactions, Kluwer Academic Publishers, The Netherlands, 1996, pp. 249–264.
[37] J. Hanley, Y. Deligiannakis, A. Pascal, P. Faller, A.W. Rutherford, Carotenoid oxidation in photosystem II, Biochemistry 38 (1999) 8189–8195.
[38] P. Faller, C. Fufezan, W.A. Rutherford, Side-path electron donors: cytochrome b_{559}, chlorophyll Z and β-carotene, in: T. Wydrzinski, K. Satoh (Eds.), Photosystem II: The Light-Driven Water: Plastoquinone Oxidoreductase, Springer, The Netherlands, 2005, pp. 347–365.
[39] K.E. Shinopoulos, J. Yu, P.J. Nixon, G.W. Brudwig, Using site-directed mutagenesis to probe the role of the D2 carotenoid in the secondary electron-transfer pathway of photosystem II, Photosynth. Res. 120 (2014) 141–152.
[40] C.A. Buser, B.A. Diner, G.W. Brudvig, Photooxidation of cytochrome b_{559} in oxygen-evolving photosystem II, Biochemistry 31 (1992) 11449–11459.
[41] N. Bondarava, C.M. Gross, M. Mubarakshina, J.R. Golecki, G.N. Johnson, A. Krieger-Liszkay, Putative function of cytochrome b_{559} as a plastoquinol oxidase, Physiol. Plant. 138 (2010) 463–473.
[42] H. Eichelmann, V. Oja, R.B. Peterson, A. Laisk, The rate of nitrite reduction in leaves as indicated by O_2 and CO_2 exchange during photosynthesis, J. Exp. Bot. 62 (2011) 2205–2215.
[43] A. Laisk, V. Oja, Dynamic gas exchange of leaf photosynthesis, Measurement and Interpretation, CSIRO, Canberra, 1998.
[44] A. Laisk, V. Oja, B. Rasulov, H. Rämma, H. Eichelmann, I. Kasparova, H. Pettai, E. Padu, E. Vapaavuori, A computer-operated routine of gas exchange and optical measurements to diagnose photosynthetic apparatus in leaves, Plant Cell Environ. 25 (2002) 923–943.
[45] V. Oja, H. Eichelmann, A. Laisk, Calibration of simultaneous measurements of photosynthetic carbon dioxide uptake and oxygen evolution in leaves, Plant Cell Physiol. 48 (2007) 198–203.
[46] V. Oja, A. Laisk, Oxygen yield from single turnover flashes in leaves: non-photochemical excitation quenching and the number of active PSII, Biochim. Biophys. Acta 1460 (2000) 291–301.
[47] R.B. Peterson, V. Oja, H. Eichelmann, I. Bichele, L. Dall'Osto, A. Laisk, Fluorescence F_0 of photosystems II and I in developing C_3 and C_4 leaves, and implications on regulation of excitation balance, Photosynth. Res. (2014)http://dx.doi.org/10.1007/s11120-14-0009-5.
[48] P. Gaastra, Photosynthesis of crop plants as influenced by light, carbon dioxide, temperature, and stomatal diffusion resistance, Mededelingen van de Landbouwhogeschool te Wageningen591959. 1–68.
[49] A. Laisk, Kinetics of Photosynthesis and Photorespiration in C_3 Plants, in, Nauka, Moscow, 1977.
[50] A. Laisk, H. Eichelmann, V. Oja, E. Talts, R. Scheibe, Rates and roles of cyclic and alternative electron flow in potato leaves, Plant Cell Physiol. 48 (2007) 1575–1588.
[51] V. Oja, H. Eichelmann, A. Laisk, Oxygen evolution from single- and multiple-turnover light pulses: temporal kinetics of electron transport through PSII in sunflower leaves, Photosynth. Res. 110 (2011) 99–109.
[52] H. Pettai, V. Oja, A. Freiberg, L. A., Photosynthetic activity of far-red light in green plants, Biochim. Biophys. Acta 1708 (2005) 311–321.
[53] A. Laisk, V. Oja, U. Heber, Steady-state and induction kinetics of photosynthetic electron transport related to donor side oxidation and acceptor side reduction of Photosystem I in sunflower leaves, Photosynthetica 27 (4) (1992) 449–463.
[54] T. Joët, L. Cournac, G. Peltier, M. Havaux, Cyclic electron flow around photosystem I in C_3 plants. In vivo control by the redox state of chloroplasts and involvement of the NADH-dehydrogenase complex, Plant Physiol. 128 (2002) 760–769.
[55] P. Joliot, A. Joliot, Cyclic electron transfer in plant leaf, PNAS 99 (2002) 10209–10214.
[56] A. Laisk, V. Oja, D. Walker, U. Heber, Oscillations in photosynthesis and reduction of Photosystem I acceptor side in sunflower leaves. Functional Cyt b/f-PSI-FNR complexes, Photosynthetica 27 (4) (1992) 465–479.
[57] D.A. Walker, Concerning oscillations, Photosynth. Res. 34 (1992) 387–395.
[58] A. Laisk, E. Talts, V. Oja, H. Eichelmann, R. Peterson, Fast cyclic electron transport around photosystem I in leaves under far-red light: a proton-uncoupled pathway? Photosynth. Res. 103 (2010) 79–95.
[59] D.I. Arnon, G.M.-S. Tsang, Cytochrome b_{559} and proton conductane in oxygenic photosynthesis, Proc. Natl. Acad. Sci. U. S. A. 85 (1988) 9524–9528.
[60] O.P. Kaminskaya, V.A. Shuvalov, G. Renger, The PSII complex possesses a quinone-binding site that differs from Q_A and Q_B and interacts with cytochrome b_{559}, Dokl. Biochem. Biophys. 412 (2007) 12–14.
[61] O.P. Kaminskaya, L.G. Erokhina, V.A. Shuvalov, Study of the nature of biphasic reduction of cytochrome b_{559} by plastoquinol in photosystem II membrane fragments, Dokl. Biochem. Biophys. 447 (2012) 273–276.
[62] A. Guskov, J. Kern, A. Gabdulkhakov, M. Broser, A. Zouni, W. Saenger, Cyanobacterial photosystem II at 2.9-A resolution and the role of quinones, lipids, channels and chloride, Nat. Struct. Mol. Biol. 16 (2009) 334–342.
[63] Y. Umena, K. Kawakami, J.-R. Shen, N. Kamiya, Crystal structure of oxygen-evolving photosystem II at a resolution of 1.9 Å, Nature 473 (2011) 55–61.
[64] O. Kaminskaya, V.A. Shuvalov, G. Renger, Evidence for a novel quinone-binding site in the photosystem II (PS II) complex that regulates the redox potential of cytochrome b_{559}, Biochemistry 46 (2007) 1091–1105.
[65] K. Hasegawa, T. Noguchi, Molecular interactions of the quinone electron acceptors Q_A, Q_B, and Q_C in photosystem II as studied by the fragment molecular orbital method, Photosynth. Res. 120 (2014) 113–123.
[66] K. Shinopoulos, G. Brudvig, Cytochrome b_{559} and cyclic electron transfer within photodsystem II, Biochim. Biophys. Acta 1817 (2012) 66–75.
[67] G. Christen, F. Reifarth, G. Renger, On the origin of the '35-μs kinetics' of $P680^+$ reduction in photosystem II with an intact water oxidizing complex, FEBS Lett. 429 (1998) 49–52.
[68] J.F. Allen, How does protein phosphorylation regulate photosynthesis? Trends Biochem. Sci. 17 (1992) 12–17.
[69] J. Lavergne, F. Rappaport, Stabilization of charge separation and photochemical misses in photosystem II, Biochemistry 37 (1998) 7899–7906.
[70] A. Malnoe, F.-A. Wollman, C. de Vitry, F. Rappaport, Photosynthetic growth despite a broken Q-cycle, Nat. Commun. 2 (2011) 301, http://dx.doi.org/10.1038/ncomms1299.
[71] P. Galka, A. Santabarbara, T.T.H. Khuong, H. Degand, P. Morsomme, R.C. Jennings, E.J. Boekema, S. Caffarri, Functional analyses of the plant photosystem I-light-harvesting complex II supercomplex reveal that light-harvesting complex II loosely bound to photosystem II is a very efficient antenna for photosystem I in state II, Plant cell 24 (2012) 2963–2978.
[72] P. Joliot, A. Joliot, Evidence for a double hit process in photosystem II based on fluorescence studies, Biochim. Biophys. Acta 462 (1977) 559–574.
[73] V. Oja, A. Laisk, Photosystem II antennae are not energetically connected: evidence based on flash-induced O_2 evolution and chlorophyll fluorescence in sunflower leaves, Photosynth. Res. 114 (2012) 15–28.
[74] B. Ivanov, M. Mubarakshina, S. Korobrykh, Kinetics of the plastoquinone pool oxidation following illumination. Oxygen incorporation into photosynthetic electron transport chain, FEBS Lett. 581 (2007) 1342–1346.
[75] M. Ribas-Carbo, J.A. Berry, J. Azcon-Bieto, J.N. Siedow, The reaction of the plant mitochondrial cyanide-resistant alternative oxidase with oxygen, Biochim. Biophys. Acta 1188 (1994) 205–212.
[76] J. Lavergne, Mitochondrial responses to intracellular pulses of photosynthetic oxygen, Proc. Natl. Acad. Sci. U. S. A. 86 (1989) 8768–8772.
[77] A. Laisk, V. Oja, H. Eichelmann, Kinetics of leaf oxygen uptake represent in planta activities of respiratory electron transport and terminal oxidases, Physiol. Plant. 131 (2007) 1–9.